Application of Parametric Reduced Order Models for Bladed Disks

Undergraduate Honors Thesis

By

Ryan Wilber

May 2017

Advisor

Dr. Kiran D’Souza

Abstract

Gas turbines experience vibration effects in blades during normal operations, however, if unchecked these vibrations can lead to failure. There are many parameters that affect these vibrations including mistuning effects, which changes the stiffness of individual blades, and rotational speed, which makes all the blades on the disk stiffer. The goal of this research is to utilize a parametric method to approximate the effects of rotational speed and mistuning while being computationally efficient. Bladed disk geometries are very complex, leading to high computational costs when running vibration simulations. For this reason, reduced order models are created in order to make the analysis more efficient. To couple the effects of these parameters, the Parametric Reduced Order Modeling method is first used to approximate the stiffness matrix at any speed by using a Taylor series approximation at three simulated speeds. The CMM method is then used to create the reduced order model using a set of the mode shapes from the vibration analysis of a single blade and disk portion. This method also is used to apply the mistuning. A forced response calculation can then be performed on this reduced system, requiring less time to compute than a full simulation. Preliminary results show that rotational effects will cause a quadratic increase in the natural frequencies of the blades and a great variation in the modes shapes. This causes the mode shapes for each speed to be included when reducing the matrices. This modeling method requires three initial simulations in order to run, which can increase the amount of computation time initially, however, when using this method as a design tool this method will allow designers to investigate a variety of mistuning levels and rotational speeds while being more computationally efficient than an explicit simulation.

Acknowledgements

I would like to take this time to thank those who helped me in through this project. First of all, I need to thank my advisor Dr. Kiran D'Souza. His leadership, knowledge, and expertise in this field helped to propel my own education in mechanical engineering. He was there to help me through a research project in vibrations, a subject that is not too detailed in many undergraduate classes, and helped me to discover the world of engineering vibrations.

I would also like to thank Eric Kurstak. His knowledge of mechanical vibrations, linear algebra, ANSYS programming, and many other subjects is what helped me to move past many roadblocks I found with this project.

I want to thank the College of Engineering at Ohio State and the Ohio Space Grant Consortium for scholarships for students involved with research.

I would also like to thank my family for their support throughout my research and educational career.

Table of Contents

Abstract……ii

Acknowledgments……..iii

List of Figures……..v

List of Tables……..vi

I. Background……..1

II. Methodology…….11

III. Results…….16

IV. Conclusions……...….....24

References…….27

List of Figures

Figure 1: Bladed disk, or Blisk, model……1

Figure 2: Example of cyclic symmetry……2

Figure 3: Model of a single sector……3

Figure 4**:** Various failure types in gas turbine blades……4

Figure 5: 1-DOF vibration system……5

Figure 6: 2-DOF vibration system……6

Figure 7: Vibration localization on a blisk……9

Figure 8: Effect on natural frequency for a single mode……17

Figure 9: Initial ANSYS procedure to extract information to create ROM……18

Figure 10: Single sector mode shape……19

Figure 11: Cyclic symmetry mode shape……20

Figure 12: New ANSYS procedure to extract information to create ROM……21

Figure 13: Tuned system PROM vs ROM at 17,500 rpm……22

List of Tables

Table 1: Computational cost for tuned system PROM creation……23

Table 2: Computational time for the reduction of the PROM terms……24

I. Background

Motivation

Highly integrated systems in engineering are described as mapping functions over multiple components in the design, causing component interdependence. A consequence of these systems is that failure in one component can cascade rapidly throughout the entire system, causing complete failure. Gas turbines are an example of this kind of system are used in very sensitive areas, such as jet engines and power plants. Total system failure in these systems when in the field can have devastating consequences and is not an option, so these systems must be tested and verified for many methods of failure.

Vibration response can have a large impact on the blades themselves in a gas turbine. The blades are a portion of a larger component, known as a bladed disk (blisk). The blades themselves and disk that they are attached to compose a full blisk, which can also be known as a stage if multiple blisks are used in a particular engine.

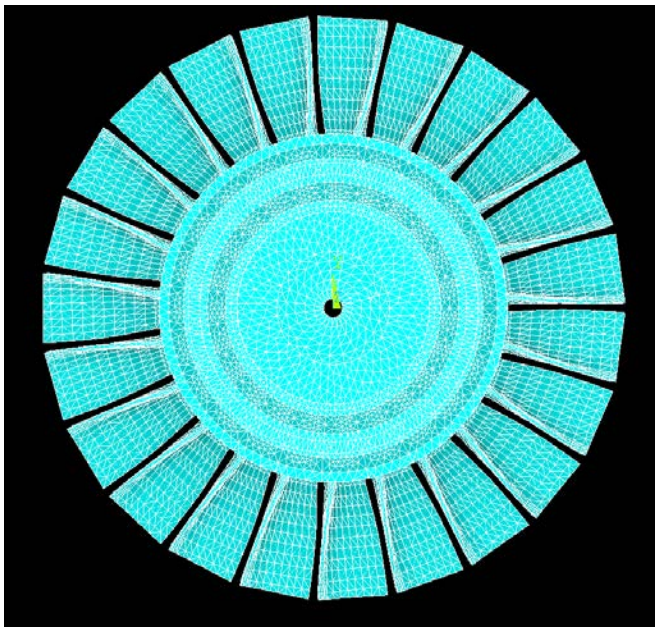

Figure 1: Bladed disk, or Blisk, model.

A blisk exhibits cyclic symmetry, which is the repetition of a single component around a common axis, therefore causing the full structure to be created. A graphic highlighting this symmetry can be seen in Figure 2. This smaller component that is repeated is known as a sector, shown in Figure 3, and is comprised of a single blade and its corresponding disk portion. The number of sectors that a particular blisk is made of is equal to the number of blades in the blisk itself.

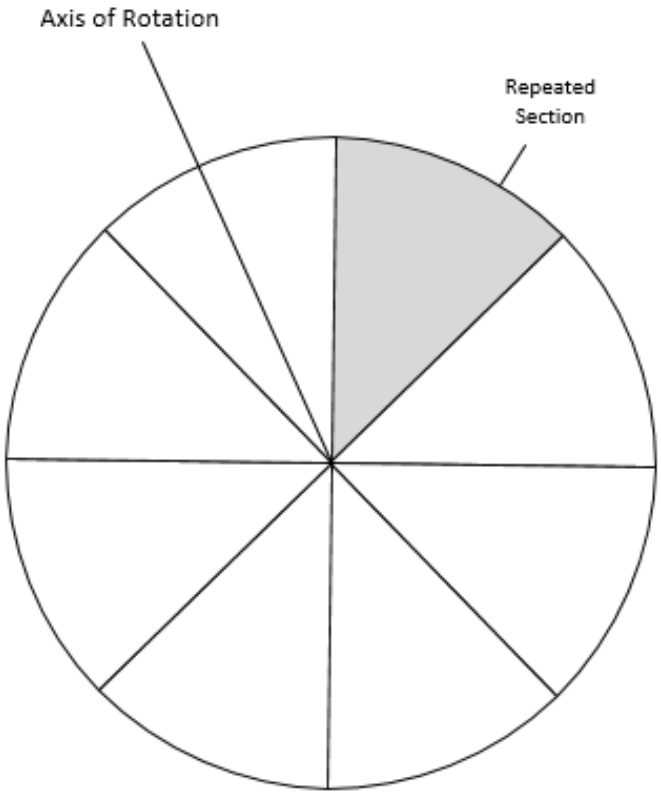

Figure 2: Example of cyclic symmetry.

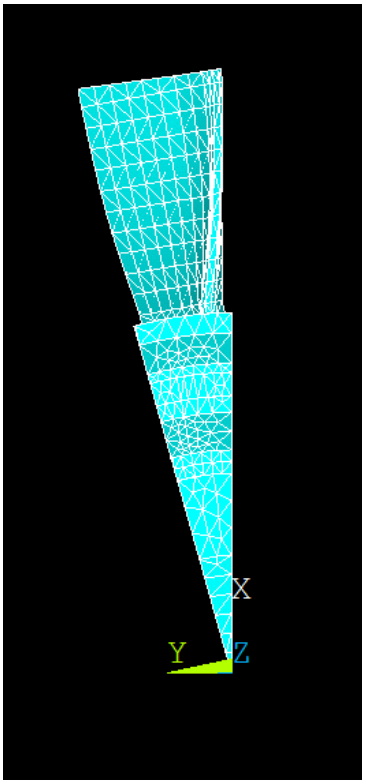

Figure 3: Model of a single sector.

As shown in the model, the blades on this disk are typically cantilevered from the disk. During operation, if the blades are excited near a natural frequency high amplitude vibrations can occur, just like a cantilever beam. This vibration, if not understood and taken into account during design, can lead to cracking in the blades and ultimately blade shearing, as seen in Figure 4. This failure of the blades could cascade throughout the entire system, causing complete turbine failure.

Figure 4: Various failure types in gas turbine blades [1].

Understanding these vibrations and the factors that affect them are critical to preventing these failures in the system. With this understanding comes the need to be able to simulate different scenarios that could affect a design for a blisk. For this task finite element analysis (FEA) programs are used in order to apply representative material properties and boundary conditions in a simulation environment and to solve for the response. Blisks are complicated geometrical structures, however, and the modeling of an entire blisk can lead to high computational costs.

An example of how large these computational costs can become can be seen with the representative academic model shown in Figure 1 and Figure 3. This academic model shows a representative shape of a bladed disk, but is simplified geometrically. The single sector of this

model contains 1246 nodes. The full stage in this system has 23 sectors, therefore the full stage has 28,658 nodes or 85974 degrees of freedom in the system. These degrees of freedom dictate the size of square matrices that need to be used to solve for the response. This is moderate sized finite element model was specifically designed for the purpose of efficiency. Actual blisk models can be well over 100,000 nodes in order to capture the full geometry of the sector itself. This large size increases the time it takes to run simulations, thus increasing the computational cost.

Vibrations and Reduced Order Modeling

Due to these large computational costs for these complex vibration problems, methods have been developed in order to approximate the responses of complex systems. To begin to develop these methods, the 1-degree of freedom (DOF) vibration problem is considered. Figure 5 shows the schematic of this problem while Equation (1) shows its equation of motion. This equation takes into account the motion of the mass only in the horizontal plane, along with the effects of the spring, damper, and external forcing on the mass.

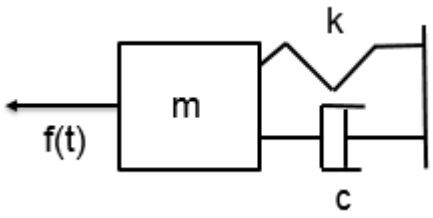

Figure 5: 1-DOF vibration system.

$$m\ddot{x} + c\dot{x} + kx = f(t) \tag{1}$$

Adding more masses to this system increases the number of degrees of freedom in the system, as both masses can move independently of each other, but are coupled by elements between them.

The equation of motions for this system shown in Figure 6 can be represented in a matrix form, as seen in Equation (2) [2].

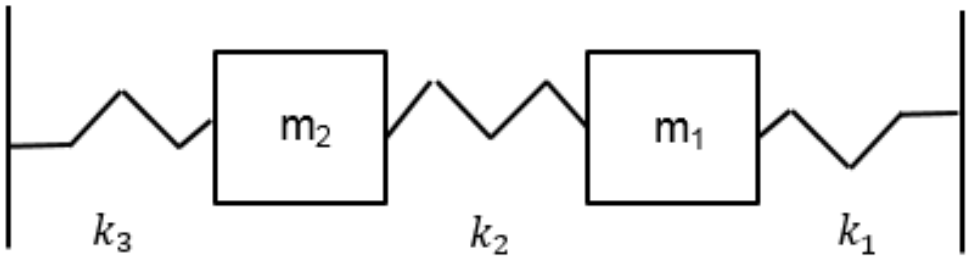

Figure 6: 2-DOF vibration system.

$$\begin{bmatrix} m_1 & 0 \\ 0 & m_2 \end{bmatrix} \ddot{x} + \begin{bmatrix} k_1 + k_2 & -k_2 \\ -k_2 & k_2 + k_3 \end{bmatrix} x = \overrightarrow{f(t)} \tag{2}$$

This representation shows a mass matrix and stiffness matrix, along with a forcing vector representing forcing on either mass. For simplicity the damping matrix was not included, but it could also be added in a similar way. For brevity, the mass matrix will be referred to as $\boldsymbol{M}$, the stiffness matrix will be referred to as $\boldsymbol{K}$, and the forcing vector will be referred to as $\boldsymbol{F}$. This leads to Equation (2) being represented as Equation (3).

$$\boldsymbol{M}\ddot{x} + \boldsymbol{K}x = \boldsymbol{F} \tag{3}$$

For further analysis, the equation above can be transferred to the frequency domain, giving Equation (4) below. This introduces $\boldsymbol{q}$, or the system response in physical coordinates.

$$\left(\boldsymbol{K} - \boldsymbol{\omega^2 M}\right)\boldsymbol{q} = \boldsymbol{F} \tag{4}$$

This representation of the system still shows the full mass and stiffness matrix of the system, which, as mentioned previously, can be very large for the full system model, as this includes

information for all degrees of freedom for each node. For this vibration analysis, only the UX, UY, and UZ directions are considered, therefore the mass and stiffness matrix are three times larger than the amount of nodes in the model. This can lead to multiple matrices of greater than 80,000 by 80,000 elements.

Because of this problem, reduced order models (ROMs) have been developed in order to reduce the size of these matrices, decreasing the amount of calculations to perform and increasing the computational speed. As shown in Lim et al. [3] constructing the ROM is done by transforming the equation and matrices to the modal coordinate system. Equations (5) and (6) shows the beginning of the reduction of the mass and stiffness matrices using the transformation matrix of eigenvectors, or mode shapes ($\boldsymbol{\Phi}$) of the system being analyzed. The eigenvectors are normalized to the mass matrix itself, meaning the reduction of the mass matrix yields the identity matrix, as seen in Equation (5). The reduction of the stiffness matrix gives the eigenvalues of the system ($\boldsymbol{\Lambda}$) [3]. Both of these components are then used in the frequency domain equation in the modal coordinate system, along with a transformation of the forcing vector as seen in Equation (7) [3]. Using this ROM, the modal coordinates of the response $\boldsymbol{p}$ are solved for. By using the same transformation matrix $\boldsymbol{\Phi}$ the solution of the forced response, and then $\boldsymbol{q}$ is computed and for forced response simulation is complete [3].

$$\boldsymbol{\Phi^T K \Phi} = \boldsymbol{\Lambda} \tag{5}$$

$$\boldsymbol{\Phi^T M \Phi} = \boldsymbol{I} \tag{6}$$

$$(\boldsymbol{\Lambda^s} - \omega^2\, \boldsymbol{I})\, \boldsymbol{p} = \boldsymbol{\Phi^T}\, \boldsymbol{F} \tag{7}$$

$$\boldsymbol{\Phi^s p} = \boldsymbol{q} \tag{8}$$

Mistuning Effects

The ROM created above highlights a basic tuned system, however, many reduced order modeling methods have been developed in the past take into account different parameters that affect the response of the blades, such as Lim et al. and Sternchüss [3, 4]. Mistuning is one such effect that refers to mass or stiffness changes in individual blades. Material properties and manufacturing variations of individual blades can introduce mistuning to a blisk, and accounting for this in simulations can give a better representation of experimental results. As explained in Castanier and Pierre [5], the amount of mistuning present varies per blade in a specific disk, and this can lead to vibration localization. Vibration localization is high amplitude vibration in only a few blades due to their mistuning, as seen in Figure 7. This localization can cause higher amplitudes of vibration than the perfectly tuned system and can cause excess fatigue and failure if they exceed the designed amplitude. Verification of blisks with the almost random mistuning effect requires simulation across many mistuning patterns and amounts. An ability to apply this mistuning quickly in the reduced space of a ROM is an area of active research and many methods have been developed to do so, such as the component mode mistuning method developed by Lim et al. discussed in Section II [3]. These efforts aim to reduce the calculation time for these forced response to save on computational costs in verification.

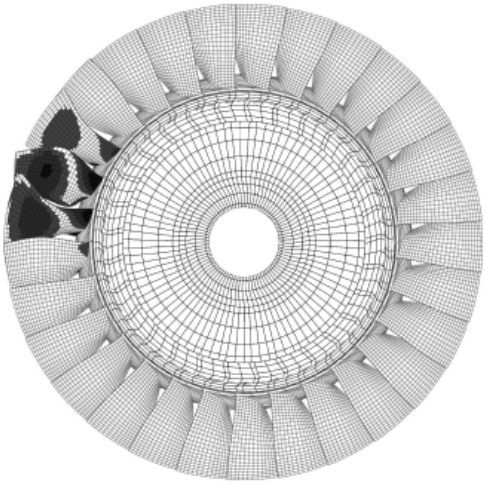

Figure 7: Vibration localization on a blisk [5].

Rotational Speed Effects

Blisks in a gas turbine spin at some operational speed or speeds when in operation. This spinning can lead to stress stiffening in the blades, as explained in Sternchüss [4] and Sreenivasamurthy and Ramamurti [6]. This stress stiffening effect causes the blades to become stiffer as rotational speed increases, increasing the natural frequency of the system. The spinning effect it taken into account by rotational matrix as seen in Equation (8) [4, 6]. For blisks, only one direction, the Z direction, is used, allowing for a simplification in the rotational matrix. The stress stiffening effects are then accounted for analytically by using matrices of the shape functions in Equation (9) and can be simply added to the initial stiffness matrix in order to find the new global stiffness matrix [4, 6]. Analytically, the inclusion of the stress stiffening effect leads to a quadratic increase in the stiffness of the blades, and therefore a quadratic increase in the natural frequencies as speed increases.

$$A_2 = \begin{bmatrix} \Omega_y^2 + \Omega_z^2 & -\Omega_x\Omega_y & -\Omega_x\Omega_z \\ -\Omega_x\Omega_y & \Omega_x^2 + \Omega_z^2 & -\Omega_z\Omega_y \\ -\Omega_x\Omega_z & -\Omega_z\Omega_y & \Omega_x^2 + \Omega_y^2 \end{bmatrix} = \begin{bmatrix} \Omega_z^2 & 0 & 0 \\ 0 & \Omega_z^2 & 0 \\ 0 & 0 & 0 \end{bmatrix} \quad (8)$$

$$K_r = \rho \int_{vol} [N]'[A_2][N] \quad (9)$$

$$K_t = K_o + K_r \quad (10)$$

The inclusion of stress stiffening effects historically was taken at the simulation level, meaning the initial stiffness matrix considered these effects. However, the newer ROMs developed by Sternchüss [4] have investigated varying the rotational speed in the reduced space.

Purpose of Research

Previous research has focused on creating ROMs to account for either the mistuning or rotational speed in the reduced case. This approach to ROM creation means that for a ROM designed to vary mistuning, a new ROM must be created at each rotational speed of interest. Likewise, for a ROM created to vary operational speed, a new ROM is needed to vary mistuning in the system. Each of these parameters could potentially be varied for a given gas turbine design and both must be analyzed when designing a blisk in order to verify the design.

This research project will develop a new method ROM coupling the effects of rotational speed and mistuning to both be varied in the reduced order space. Doing so would allow for a more comprehensive ROM to be created and improve computational efficiency when designing blisks by reducing the amount of ROMs that are required.

Section II will explore two different preexisting modeling methods and combine them into a new methodology for creating reduced order models. Section III will present the results from this new

ROM and compare the forced response to the original ROMs as well as full simulations of the blisk. Section IV presents the conclusions of the research, as well as future work to further develop this method.

II. Methodology

Parametric Reduced Order Modeling

Previous methods have been developed by Sternchüss [4] for applying rotational speed in the reduced space in order to account for changes in stiffness at new rotational speeds. The application for applying this change in speed is the parametric reduced order models (PROMs) developed by Hong et al [7]. The PROM method uses Taylor Series approximations in order approximate the mass and stiffness matrices for a change in a specific parameter. This allows for a mass matrix to be varied along with stiffness matrices, however, from Sternchüss [4] and Sreenivasamurthy and Ramamurti [6] only the stiffness matrix varies with rotational speed. The Taylor Series approximation from Hong et al. to vary the stiffness matrix as the parameter $\boldsymbol{p}$ varies is shown in Equation (11) [7].

$$\boldsymbol{K_i}(p) \approx \boldsymbol{K_i}(p_0) + \frac{\partial \boldsymbol{K_i}}{\partial p}(p - p_0) + \frac{1}{2}\frac{\partial^2 \boldsymbol{K_i}}{\partial p^2}(p - p_0)^2 + \frac{1}{6}\frac{\partial^3 \boldsymbol{K_i}}{\partial p^3}(p - p_0)^3 \tag{11}$$

The rotational matrix seen in Equation (8) shows that as the rotational speed increases, the stiffness values should increase quadratically [4, 6]. Due to this, only the second derivative of the Taylor Series approximation is required to accurately capture the stress stiffening effect. The partial derivatives with respect to the parameter are able to be computed as finite difference formulas. Investigation into this method has determined that for the first finite derivative, a truncation error of at least $O(h^2)$ is required to accurately capture the stiffness changes, leading to

Equation (12). The truncation error for the second finite derivative is able to be on the order of O(h), leading to Equation (13).

$$\boldsymbol{K_{FD}^{1}} = \frac{-\boldsymbol{K_i}(p_0 + 2\Delta p) + 4 * \boldsymbol{K_i}(p_0 + \Delta p) - 3 * \boldsymbol{K_i}(p_0)}{2 * \Delta p} \tag{12}$$

$$\boldsymbol{K_{FD}^{2}} = \frac{1}{2}\frac{\boldsymbol{K_i}(p_0 + \Delta p) - 2\boldsymbol{K_i}(p_0) + \boldsymbol{K_i}(p_0 - \Delta p)}{\Delta p^2} \tag{13}$$

$$\boldsymbol{K_i}(p) \approx \boldsymbol{K_i}(p_0) + \boldsymbol{K_{FD}^{1}}(p - p_0) + \frac{1}{2}\boldsymbol{K_{FD}^{2}}(p - p_0)^2 \tag{14}$$

Equation (14) shows the full approximation of the stiffness matrix to the system, where the parameter being varied is rotational speed of the system in rpm. However, this stiffness does not need to be computed in full, but can be reduced on a term by term bases to increase computational efficiency.

In order to create a ROM a transformation matrix that includes information from each rotational speed. A methodology proposed in Hong et al. [7] is used to create an augmented $\boldsymbol{\Phi}$ matrix from each of the operational speeds used in the approximation.

$$\boldsymbol{\Phi_{aug}} = [\boldsymbol{\Phi_1}\ \boldsymbol{\Phi_2}\ \boldsymbol{\Phi_3}] \tag{15}$$

The modes shapes in this equation are not orthogonal and an orthogonal basis is approximated for use as a transformation matrix [7]. This matrix $\boldsymbol{U}$ is formed from the left singular modes that correspond to a singular values of at least 0.01% of the maximum singular value in a singular value decomposition of $\boldsymbol{\Phi_{aug}}$ [7]. This matrix is then able to be used to create the reduced order model for the system. This reduction gives the eigenvalues of the system at the new specified

speed, $\boldsymbol{\Lambda_0}(p)$, and the identity matrix when reducing mass, due to the mode shapes being normalized to the mass matrix.

$$\boldsymbol{\Lambda_0}(p) \approx \boldsymbol{U^t K_i}(p_0)\boldsymbol{U} + \boldsymbol{U^t K_{FD}^1 U}(p - p_0) + \frac{1}{2}\boldsymbol{U^t K_{FD}^2 U}(p - p_0)^2 \tag{16}$$

$$\boldsymbol{I} = \boldsymbol{U^t M U} \tag{17}$$

The creation of a PROM does have inherent limitations to the computational efficiency for the methodology. Mass and stiffness matrices and modes shapes at three separate rotational speeds spanning the operational range are required and must be extracted from FEA software. The reduction of each term in the Taylor series is also computationally intensive. After the PROM creation the operational speed can be varied to any value quickly in the reduced space, allowing computational saving after the initial costs. Previous ROM method would require a new ROM to be created at each operational speed, meaning if more than three speeds are to be considered, the PROM creation is more efficient.

Component Mode Mistuning

The Component Mode Mistuning (CMM) method described in Lim et al. [3] was developed as a ROM to apply mistuning in the reduced space while using cantilever blade modes to calculate the participation factors related to the blade portion of the blisk. This method served as the basis to apply mistuning to the PROM developed previously. Cantilever blades modes are calculated from a single sector, constraining the disk while allowing the blade to vibrate. The mistuning in this system was applied using the method shown in Equation (18) [3].

$$\boldsymbol{\Lambda_\delta} = \sum_{n=1}^{N} \boldsymbol{q_n^{k^t} k_{\delta,n} q_n^k} \tag{18}$$

$$\boldsymbol{k_{\delta,n}} = \boldsymbol{\Lambda_n^B} - \boldsymbol{\Lambda_o^B} \tag{19}$$

By using the cantilever blade modes, $\boldsymbol{\Phi_o^B}$, the eigenvalues of each blade, $\boldsymbol{\Lambda_n^B}$, the eigenvalues of the tuned cantilever blade, $\boldsymbol{\Lambda_o^B}$, and the stiffness participation factors, $\boldsymbol{q_n^k}$, the mistuned eigenvalues for the system, $\boldsymbol{\Lambda_\delta}$, can be computed. This can then be added to the tuned reduce stiffness matrix and can then be used in the forced response equation, completing the process for applying the mistuning in the reduced space. The procedure outlined in Equations (12)-(14) are used in order to calculate the tuned and mistuned cantilever blade eigenvalues of the system.

$$\boldsymbol{\Lambda_{FD,o}^1} = \frac{-\boldsymbol{\Lambda_o^B}(p_0 + 2\Delta p) + 4 * \boldsymbol{\Lambda_o^B}(p_0 + \Delta p) - 3 * \boldsymbol{\Lambda_o^B}(p_0)}{2 * \Delta p} \tag{20}$$

$$\boldsymbol{\Lambda_{FD,o}^2} = \frac{1}{2}\frac{\boldsymbol{\Lambda_o^B}(p_0 + \Delta p) - 2\boldsymbol{\Lambda_o^B}(p_0) + \boldsymbol{\Lambda_o^B}(p_0 - \Delta p)}{\Delta p^2} \tag{21}$$

$$\boldsymbol{\Lambda_o^B}(p) \approx \boldsymbol{\Lambda_o^B}(p_0) + \boldsymbol{\Lambda_{FD,o}^1}(p - p_0) + \frac{1}{2}\boldsymbol{\Lambda_{FD,o}^2}(p - p_0)^2 \tag{22}$$

$$\boldsymbol{\Lambda_{FD,\delta}^1} = \frac{-\boldsymbol{\Lambda_\delta^B}(p_0 + 2\Delta p) + 4 * \boldsymbol{\Lambda_\delta^B}(p_0 + \Delta p) - 3 * \boldsymbol{\Lambda_\delta^B}(p_0)}{2 * \Delta p} \tag{23}$$

$$\boldsymbol{\Lambda_{FD,\delta}^2} = \frac{1}{2}\frac{\boldsymbol{\Lambda_\delta^B}(p_0 + \Delta p) - 2\boldsymbol{\Lambda_\delta^B}(p_0) + \boldsymbol{\Lambda_\delta^B}(p_0 - \Delta p)}{\Delta p^2} \tag{24}$$

$$\boldsymbol{\Lambda_\delta^B}(p) \approx \boldsymbol{\Lambda_\delta^B}(p_0) + \boldsymbol{\Lambda_{FD,\delta}^1}(p - p_0) + \frac{1}{2}\boldsymbol{\Lambda_{FD,\delta}^2}(p - p_0)^2 \tag{25}$$

To calculate the participation factors of the, the blade portion of the transformation matrix, $\boldsymbol{U}$, is extracted in cyclic coordinates per harmonic. This matrix, $\widetilde{\boldsymbol{U}}_{b,h}$, is used in order to find the cyclic participation factors, $\widetilde{\boldsymbol{q}}_h^k$. Following the same process for finding the transformation matrix $\boldsymbol{U}$ the cantilever blade transformation matrix $\boldsymbol{U^B}$ must also be calculated. These sets of information lead us to the resulting

equation, modified from Lim et al. [3], to solve the for the participation factors. The cantilever blade stiffness values must also be found at the three base speeds and interpolated using the exact same procedure as before.

$$\tilde{\boldsymbol{q}}_h^k = \boldsymbol{\Lambda^B}(p)^{-1}\left(\begin{bmatrix}\boldsymbol{U^B}\\ \boldsymbol{0}\end{bmatrix}^t \boldsymbol{K^B}(p_0)\tilde{\boldsymbol{U}}_{b,h} + \begin{bmatrix}\boldsymbol{U^B}\\ \boldsymbol{0}\end{bmatrix}^t \boldsymbol{K_{FD}^{B,1}}\tilde{\boldsymbol{U}}_{b,h}(p-p_0) + \frac{1}{2}\begin{bmatrix}\boldsymbol{U^B}\\ \boldsymbol{0}\end{bmatrix}^t \boldsymbol{K_{FD}^{B,2}}\tilde{\boldsymbol{U}}_{b,h}(p-p_0)^2\right) \tag{26}$$

This representation of the participation factors are in cyclic coordinates. In order to extract the participation factors for each blade in physical coordinates, the cyclic participation factors are multiplied using the Fourier matrix $\boldsymbol{F}$ and the Kronecker Product, as seen in Equation (27). These participation factors are then used in Equation (18) to apply the mistuning in the reduced space.

$$\begin{bmatrix}\vdots\\ \boldsymbol{q_n^k}\\ \vdots\end{bmatrix} = (\boldsymbol{F}\otimes\boldsymbol{I})\boldsymbol{B}\boldsymbol{diag_h}(\tilde{\boldsymbol{q}}_h^k) \tag{27}$$

Forced Response

The forced response results for the system can be computed using Equation (28). This system solves for the response of the nodes used in model coordinates, $\boldsymbol{p}$. The damping in the system is applied by the γ term, while the mistuning is applied by adding the tuned and mistuned full system level eigenvalues together. This system requires the reduction of the forcing vector of the nodes that are excited using the transformation matrix $\boldsymbol{U}$.

$$\boldsymbol{p} = (\boldsymbol{U^t F})^{-1}\left(-\omega^2\boldsymbol{I} + (1+j\gamma)\left(\boldsymbol{\Lambda_\delta}(p) + \boldsymbol{\Lambda_0}(p)\right)\right) \tag{28}$$

Using Equation (28), a frequency sweep in forcing can then be performed to view how the mistuning and rotational effects would change the frequency response of the full system. The

modal response of the system, $\boldsymbol{p}$, must first be expanded back into the global coordinate system. This is done using Equation (29).

$$\boldsymbol{q} = \boldsymbol{U} * \boldsymbol{p} \tag{29}$$

This methodology that was developed is able to vary both the mistuning and speed in the reduced space of a single ROM and approximate the full system response due to some forcing at different frequencies. This methodology was tested, the process and results of which are explained in the following section.

III. Results

Operational Speed Variation

Sternchüss [4] and Sreenivasamurthy and Ramamurti [6] showed that the relation between rotational speed and stiffness of a blade should be quadratic, as seen in Equation (8)-(10). The simulation results were first tested against this expectation to ensure information required to construct the PROM would developed in Section II would be accurate enough to approximate the system. As shown in Equation (5) the stiffness matrix for a blisk directly relates to eigenvalues from which the natural frequencies can be directly computed. This relation allowed for the natural frequencies of the system to be extracted at different rotational speeds in order to see how the speed affected the stiffness of the blades. The natural frequencies of each mode were compared across these speeds and plotted to find their relation. An example plot at a single mode can be seen in Figure 8.

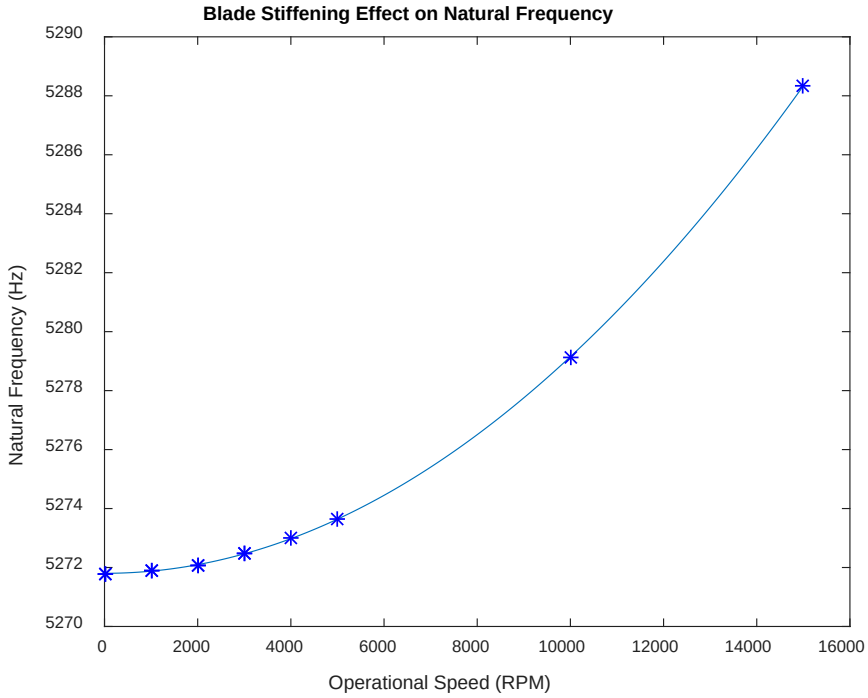

Figure 8: Effect on natural frequency for a single mode.

Each natural frequency analyzed showed a quadratic increase in natural frequency, which allowed the use of only a second derivative in the PROM creation. This also ensured that the application of the operational speed in the finite element simulation agreed with the expected theoretical trends.

Finite Element Analysis Model

The finite element model used was a simplified sector of a bladed disk, shown in Figure 3 of Section I. This simplified model had representative geometry for a bladed disk, but featured less nodes in order to increase the speed the FEA calculations required to extract needed information to create the reduced order model. This model had 1246 nodes for the single sector and 23 sectors for the full bladed disk. The elements were solid, tetrahedral elements.

Finite Element Analysis Extraction

ANSYS Mechanical was used in order to extract the needed mode shapes, mass, and stiffness matrices to construct the PROM. The process for extracting this information in ANSYS followed the flow chart seen in Figure 9. This process used two separate analyses for extracting the needed information. In order to calculate the mode shapes for the system, a cyclic analysis was required. This boundary constraint creates a second set of sector geometry in order to complete both the sine and cosine components of the wave equation. The cyclic boundary condition also applies constraints to the nodes between sectors in order to constrain their motion to match their responses in the full system. This double geometry and coupling meant that the single sector mass and stiffness matrix could not be extracted from this analysis. Therefore, a separate analysis was used without applying the cyclic boundary constraint to extract this information.

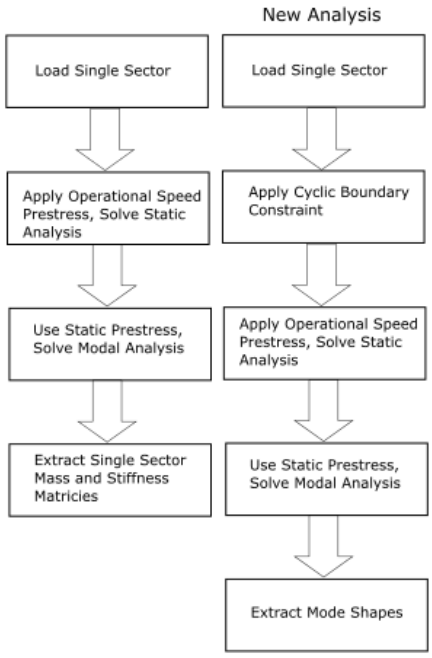

Figure 9: Initial ANSYS procedure to extract information to create ROM.

This extracted information was tested by checking the eigenvalues and identity matrix after reducing the mass and stiffness matrix using the mode shapes. Each of these matrices were expected to be diagonal, with the off diagonal terms being close to zero. This analysis worked for no rotational speed, however, it was seen that the off diagonal terms in the stiffness matrix were larger than acceptable.

The cause of this difference was determined to be the lack of the ‘High’ and ‘Low”, or intersector, boundary constraints with the prestressing effects. A contour of the displacement of a single sector analysis was plotted, seen in Figure 10, and compared to the displacement of a cyclic analysis, seen in Figure 11. From these graphs, it was seen then when the prestressing effects are applied without a cyclic boundary constraint, the ‘High’ and ‘Low’ nodes do not behave a way that is physically representative of being constrained in a disk. It was determined that the stiffness matrix from an extraction without cyclic boundary constraints at a rotational speed did not correlate to mode shapes from a cyclic analysis.

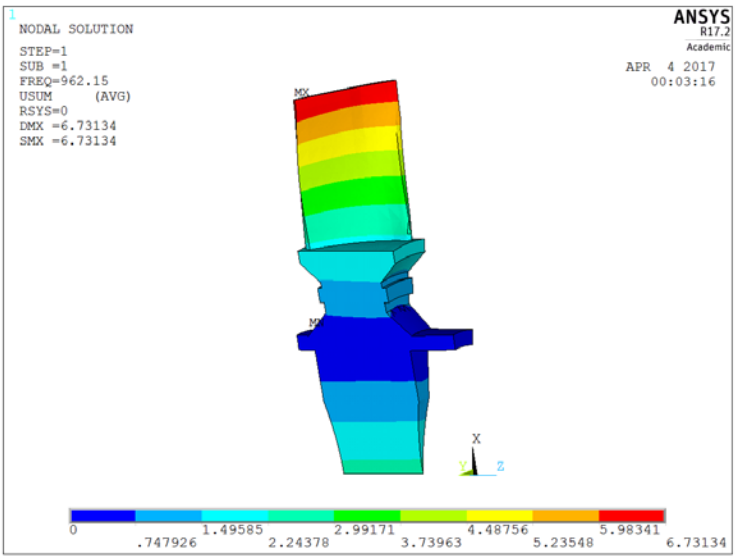

Figure 10: Single sector mode shape.

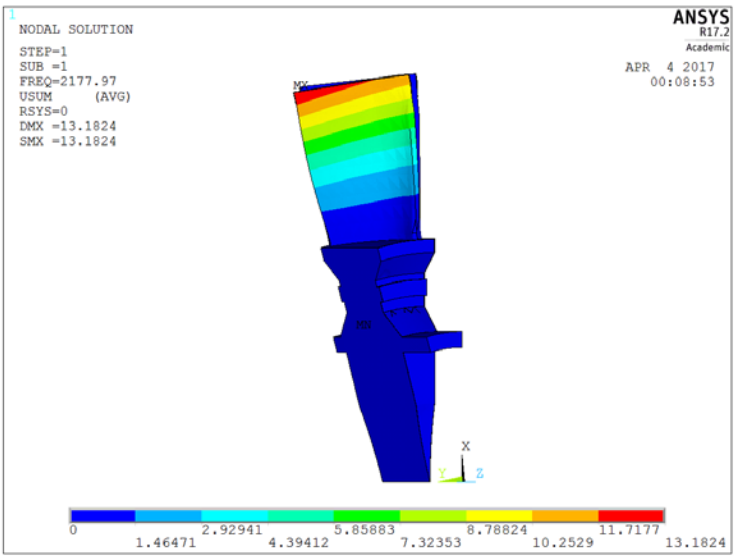

Figure 11: Cyclic symmetry mode shape.

A new method for applying the boundary constraint was developed in order to correctly match the cyclic mode shapes and a single sector mass and stiffness matrix. The procedure can be seen in Figure 12.This method applied the cyclic boundary constraint to the model in both cases. However, it did not fully couple the mass and stiffness matrix when it was required to extract those values. This created the double geometry in block diagonal form in the mass and stiffness matrices, but without coupling a submatrix could be extracted for a single sector. To extract the mode shapes of the system, the coupling was fully implemented.

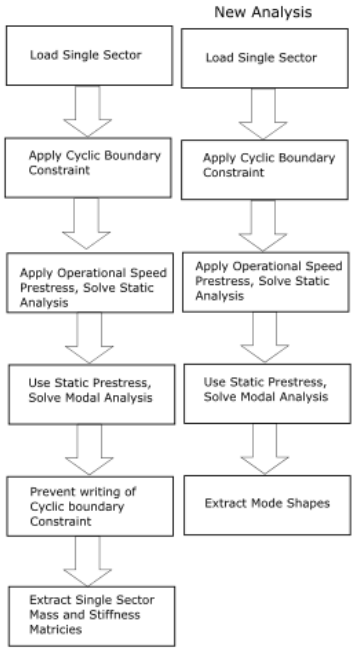

Figure 12: New ANSYS procedure to extract information to create ROM.

The agreement between the mode shapes and matrices improved with this process, with the off diagonal terms of the stiffness matrix being closer to zero than previously seen. This improvement was determined to be enough to construct the PROM.

Tuned System PROM

Using the methodology presented in Section II, a PROM was constructed with the FEA model that was presented previously. The three speeds used to construct the PROM was 0 rpm, 10,000 rpm, and 20,000 rpm. This allowed speed to be interpolated from 0-20,000 rpm. This range was chosen to allow enough of an increase in blade stiffness due to the stress stiffening effects to cause noticeable changes. The target speed for the PROM was 17,500 rpm. A regular ROM formed explicitly at 17,500 was also created for comparison to the PROM. A forced response

was performed using a forcing of 1 N at frequencies of 1000-3000 Hz at a node on the blade tip. The damping was 0.001 N-s/m. The results for the maximum response of the system at each frequency in the global coordinate system can be seen in Figure 13.

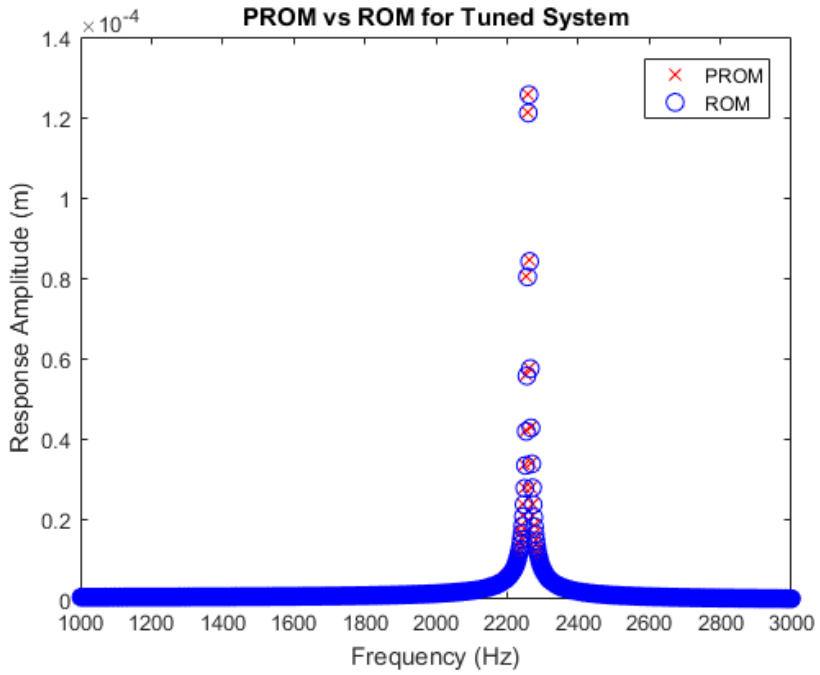

Figure 13: Tuned system PROM vs ROM at 17,500 rpm.

By visual inspection, PROM that was created matched the traditional ROM response nearly identically. The peak response at the resonant frequency had a $7.9*10^{-4}$ % difference between the two methods, showing that the PROM was able to match the ROM that was constructed specifically at the target speed. The responses also needed to match the natural frequency of this system at the excited harmonic. This corresponded to the engine order that the system was excited at, which in this analysis was the first harmonic. This harmonic had a natural frequency of 2260.86 Hz. The expected results from the reduced order models was that the system would have a resonant frequency near this natural frequency, but not exactly matching due to the damping in the system. The response for both the PROM and ROM had the peak response at

2261.72 Hz. This is a difference of 0.86 Hz, and verifies the expected trend for this system response.

The time elapsed for the steps in the PROM creation was also computed as a way to quantify the computational costs of the method. These results were done on the same computer and show sections of the creation that are computationally inefficient. This is shown in Table 1, which features the time following the extraction of mass, stiffness, and mode shape matrices from a FEA software.

Table 1: Computational cost for tuned system PROM creation.

PROM Time Breakdown	
Task	**Time (seconds)**
PROM Creation and Forced Response	
Matrix Loading/Reformatting	3.632
Finite Derivative 1	0.017
Finite Derivative 2	0.014
ROM Creation	50.446
Forcing Application	0.054
Forced Reponse	4.452
Total PROM/Forcing Time	**58.615**
Transformation Matrix Calculation	
U-Matrix Construction	**124.51**
Tranformation/PROM/Forced Response	
Total Time	**183.125**

The largest computation time was the creation of the ***U*** matrix at 124.51 seconds. This is a one-time calculation for a particular PROM due to the speeds extracted not changing and represents a single computational cost. The next largest computational cost came from the creation of the ROM itself from the ***U*** matrix and the stiffness matrices at 50.45 second. The reason for this large time was the reduction of the finite derivative terms and the initial stiffness matrix with the ***U*** matrix itself. These reduction times are shown in Table 2. For a particular set of matrices at

three speeds, these also represent one time calculations, meaning that to compute the PROM at a new rotational speed the computational time would be reduced from its initial time of 58.615 seconds, or 0.01% of the initial computation time.

Table 2: Computational time for the reduction of the PROM terms.

Reduction of PROM Terms	
Term	**Time (%)**
Initial Stiffnes at p_0	21.60
First Finite Derivative	22.05
Second Finite Derivative	23.20
Mass Matrix	20.88
U Matrix Assembly	12.26
Reduction Equation	0.01

These results for the creation of the PROM show that the main high computational costs for this method are one-time costs and after they are computed, the computational time for the PROM creation is low compared to FEA forced response simulation. These simulations can take multiple hours or days, so a method that can compute these results on the order of seconds or minutes is much more computationally efficient.

IV. Conclusions

The purpose of this research project was to utilize the parametric reduced order modeling method to apply rotational speed in the reduced space. This was to account for the stress stiffening effects causing the blades to become stiffer as speed increased. A new methodology was to be developed in order apply the component mode mistuning method to apply mistuning in the reduced space as well. This new methodology would increase the computational efficiency for conducting forced response calculations, allowing it to be used as a means to verify bladed disk designs.

The PROM was able to be constructed and applied to vary the speed of a bladed disk from the reduced space. This PROM was able to approximate the stiffness matrix at a new rotational speed accurately enough to be nearly identical to a ROM that was created explicitly at that size. The main computational costs in creating the PROM were one time calculations, the creation of the transformation matrix and its use to reduce the terms of the Taylor series. After these high initial costs, the forced response could be calculated at new rotational speed on the order of seconds. These results show good improvement over finite element analysis forced response simulation, which can take multiple hours per speed.

The methodology to apply the mistuning to this system was developed using the CMM method as a basis. This addition required the addition of cantilever blade information in order to project the mistuning of the blades in the reduced space. The methodology also required that more Taylor series be computed as the cantilever blade information also varied with rotational speed due to stress stiffening effects. Due to time constraints, the implementation of this methodology into software was not completed.

This paper has presented a methodology that allows for more than one parameter that affects the vibration response of a bladed disk in the reduced space. This methodology can be used to assist in the design stage verification at different operation conditions, allowing for the design of safer, more reliable bladed disks.

Future Work

Extensions of this research that are already being performed include the addition of the mistuning methodology that was developed to be implemented into software. This would allow this methodology to be compared to previously developed mistuning methods in accuracy and computational time at different rotational speeds. Both the tuned and mistuned system will also

be compared to full FEA simulations. This will benchmark both their accuracy as well as computational times.

Extensions to this methodology could include inclusion of parametric changes to the geometry of the bladed disks in the reduced space. This would follow the proposed use for PROMs in Hong et al. [7] in that both the mass and stiffness would need to be approximated using Taylor series. These geometric changes could be used in order to simulate geometric mistuning, or mistuning caused by variations in the shapes of the bladed disks. This could also apply to chip placement in blades or size of defects, but more research on the effects that these features have on vibrations would need to be performed. This could also be used as a design tool to vary design parameters, such as blade thickness, in the reduced space to attenuate a vibration response as a particular frequency. The inclusion of these parameters would increase the computational costs for the ROM creation due to the inclusion of varying the mass matrix and potentially requiring more terms in the Taylor series. Even with these costs, the potential to expand this methodology could allow for the creation of ROMs that could be utilized as designed tools in the construction of bladed disks.

References

[1] SWRI. (1996) Gas Turbine Technology [Online]. Available: http://www.swri.org/3pubs/brochure/d04/turbn/turbn.htm

[2] Introduction to vibration of systems with many degrees of freedom, [Online]. Available: http://www.brown.edu/Departments/Engineering/Courses/En4/Notes/vibrations_mdof/vibrations_mdof.htm

[3] Lim, S.H., Bladh, R. Castanier, M. P., Pierre, C., "Compact, Generalized Component Mode Mistuning Representation for Modeling Bladed Disk Vibration," AIAA Journal, Vol. 45, No. 9, 2007, pp. 2285-2298.

[4] Sternchüss, A., "Multi-level parametric reduced models rotating bladed disk assemblies" Ph.D. Thesis. Ecole Centrale des Arts et Manufactures, Paris, France, 2009.

[5] Castanier, M.P., Pierre, C., "Modeling and Analysis of Mistuned Bladed Disk Vibration: Status and Emerging Directions", Journal of Propulsion and Power, Vol. 22, No. 2, 2006, pp. 384-396.

[6] Sreenivasamurthy, S., and Ramamurti, V., "A Parametric Study of Vibration of Rotating Pre-Twisted and Tapered Low Aspect Ratio Cantilever Plates," Journal of Sound and Vibration Vol. 76 No. 3, 1981, pp. 311-328.

[7] Hong, S.K., Epureanu, B. I., Castanier, M. P., Gorisch, D. J. "Parametric reduced-order models for predicting the vibration response of complex structures with component damage and uncertainties," Journal of Sound and Vibration, Vol. 330, 2011, pp 1091-1110.